Düzce University Journal of Science & Technology

Antioxidant Activity and Theoretical Profile of Novel 2,4,6-Triarylpyridine Derivatives Based on Syringaldehyde

Esra Nur ALBAYRAK [a], Samed ŞİMŞEK [b], Ahmad Badreddin MUSATAT [a,c], Zeynep AKŞİT [d], Hüseyin AKŞİT [b], Alparslan ATAHAN [a,*]

ᵃ Department of Chemistry, Faculty of Art and Sciences, Düzce University, Düzce, TÜRKİYE
ᵇ Department of Basic Pharmacy Sciences, Faculty of Pharmacy, Erzincan Binali Yıldırım University, Erzincan, TÜRKİYE
ᶜ Department of Chemistry, Faculty of Sciences, Sakarya University, Sakarya, TÜRKİYE
ᵈ Vocational School of Tourism and Hotel Management, Department of Hotel, Restaurant and Catering Services, Cookery, Erzincan Binali Yıldırım University, Erzincan, TÜRKİYE
* Sorumlu yazarın e-posta adresi: alparslanatahan@duzce.edu.tr
DOI: 10.29130/dubited.1320385

ABSTRACT

Eight novel 2,4,6-triarylpyridines derived from syringaldehyde were designed and synthesized via a multicomponent one-step preparation method. Those compounds were evaluated for their antioxidant activities comparing with known reference compounds. In the studied series, toluyl, methoxyphenyl, and pyridinyl-bearing derivatives exhibited considerable antioxidant activities. Meanwhile, using the B3LYP theory and SVP, TZVP basis sets, a comprehensive theoretical quantum computing approach for the synthesized compounds was established and electronic structure descriptive parameters called Fukui indices describing the radical scavenging potential were determined. Finally, the structure-activity relationship was revealed by comparing the theoretical and experimental outputs. As a result, the potential antioxidant activity of the studied compounds was also supported by a theoretical approach.

Keywords: Triarylpyridine, Syringaldehyde, Antioxidant, DFT, Fukui indices,

Siringaldehit Bazlı Yeni 2,4,6-Triarilpiridin Türevlerinin Antioksidan Aktiviteleri ve Teorik Profili

ÖZ

Siringaldehitten türetilen sekiz adet yeni 2,4,6-triarilpiridin tasarlandı ve tek basamaklı multi-komponent yöntemle sentezlendi. Bu bileşiklerin antioksidan aktiviteleri bilinen referans bileşiklerle kıyaslanarak değerlendirildi. Çalışılan seride, toluil, metoksifenil ve piridinil taşıyan türevler dikkate değer antioksidan aktivite sergiledi. Daha sonra, B3LYP teorisi ve SVP, TZVP temel setleri kullanılarak, sentezlenen bileşikler için kapsamlı bir teorik kuantum hesaplama yaklaşımı oluşturuldu ve radikal yakalama potansiyelini tanımlayan Fukui indeksleri adlı elektronik yapı tanımlayıcı parametreler belirlendi. Son olarak, teorik ve deneysel sonuçlar karşılaştırılarak yapı-etkinlik ilişkisi ortaya konuldu. Sonuç olarak, elde edilen bileşiklerin antioksidan aktivite potansiyeli teorik bir yaklaşımla da desteklendi.

Anahtar Kelimeler: Triarilpiridin, Siringaldehit, Antioksidan, DFT, Fukui indeksi

I. INTRODUCTION

Oxidative stress, caused by excessive oxidation, plays a pivotal role in various pathological processes, including neurodegenerative disorders, cardiovascular diseases, and cancer [1,2]. In general, oxidative stress arises when there is a disturbance in the equilibrium between the production of reactive oxygen species (ROS) and the body's antioxidant defense mechanisms' ability to effectively neutralize them. This imbalance leads to the accumulation of ROS, which can result in cellular damage and contribute to various health-related issues [3]. This can lead to cell damage and has been linked to numerous diseases such as cardiovascular disease, cancer, neurodegenerative disorders, and diabetes [4-7]. Therefore, the search for natural and synthetic antioxidants is crucial in maintaining and promoting human health. Among the diverse array of natural and synthetic antioxidants, syringaldehyde and its derivatives have garnered considerable attention owing to their remarkable antioxidant properties [8-10]. Syringaldehyde, a naturally occurring compound found in a wide range of plants, has been extensively studied for its diverse biological activities. Its derivatives have been shown to possess various beneficial properties, including anti-inflammatory, anticancer, and potent antioxidant activities [11-13]. As a result, the search for antioxidant compounds has expanded to various fields of research, including nutrition, pharmacology, and biotechnology. In nutrition, researchers are investigating the antioxidant capacity of different foods and dietary supplements, with the goal of identifying dietary patterns and individual nutrients that can help prevent chronic diseases [14]. In pharmacology, researchers are exploring the potential of antioxidant compounds as therapeutic agents for various diseases. For example, some studies have shown that antioxidants such as vitamin E, vitamin C, and beta-carotene may reduce the risk of developing cardiovascular disease [15]. On the other hand, some phenolic compounds, for example, Trolox, BHA, and BHT, are known as reference antioxidant compounds in laboratory experiments [16,17]. The importance of syringaldehyde comes from its structural similarity to these compounds (Figure 1).
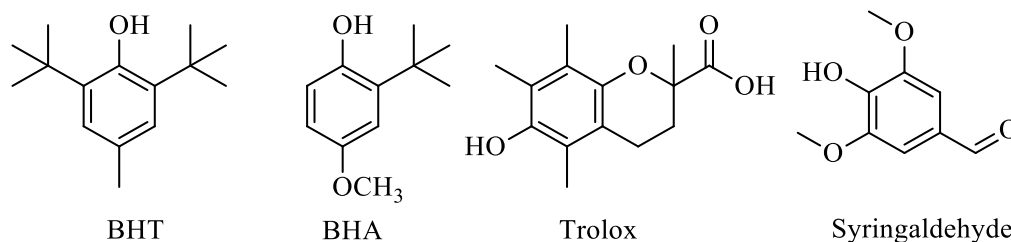

Figure 1. Structural similarity of syringaldehyde to common antioxidants

On the other hand, over the past two decades, density functional theory (DFT) has emerged as a widely embraced reliable tool for predicting molecular properties and providing a qualitative explanation for various findings in the fields of chemistry and biology. The success of DFT lies in its relatively low computational cost and improved accuracy compared to traditional quantum chemical methods. In addition, DFT has the advantage of formulating reactivity parameters, such as Fukui function, chemical hardness, electronegativity, and softness, which provide insights into molecular behavior and reactivity [18,19]. Basically the antioxidant mechanism could be evaluated theoretically by three different well-known mechanisms as HAT, SPLET and SET-PT. Those mechanisms defining O-H dissociation are usually used in various studies to evaluate the antioxidant role [20]. Herein, we singled out FUKUI indexes based on the novelty and the extraordinary role that we approach and keep with new updates in scientific methodologies. Meanwhile, this makes DFT an indispensable tool for the design and development of new molecules with desired properties, including antioxidant activity. In this article, we described the facile synthesis and characterization of novel syringaldehyde derivatives using ^{1}H-NMR, ^{13}C-NMR FT-IR techniques and evaluate their antioxidant potential using various in vitro assays, including DPPH (2,2-diphenyl-1-picrylhydrazyl) radical scavenging activity, FRAP (ferric reducing antioxidant power), and ABTS (2,2'-azinobis(3-ethylbenzothiazoline-6-sulfonic acid) radical cation) assays. Additionally, we have conducted theoretical studies using quantum calculations by evolving the density function theory using B3LYP as a base set and 2 different solvent systems to elucidate the structure-activity relationship of the synthesized derivatives and to develop a comprehensive approach

toward those newly synthesized derivatives. In summary, this study aims to contribute to the development of novel antioxidant agents based on novel syringaldehyde derivatives. The findings of this study will not only enhance our understanding about the structure-activity relationship of syringaldehyde derivatives but also provide valuable insights for the future design of new and more potent antioxidants in this field.
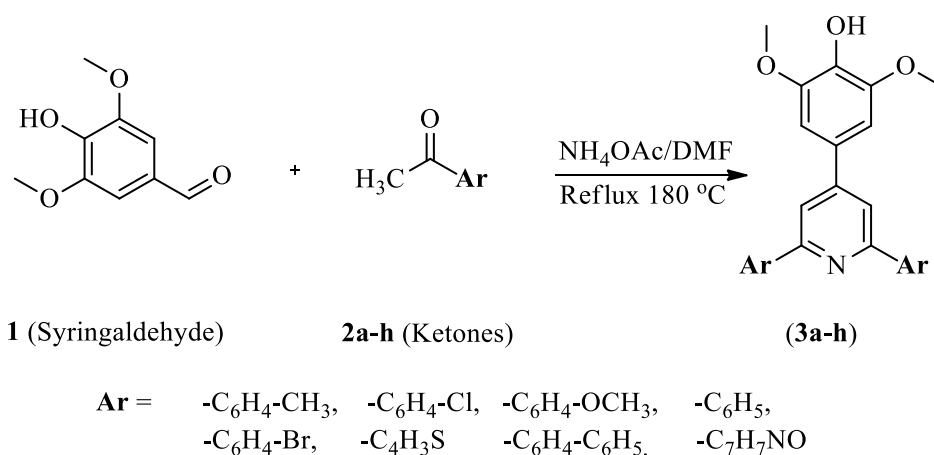
II. MATERIALS AND METHODS

A. MATERIALS

The chemicals utilized in this study were procured commercially from reputable sources, namely Merck, Sigma-Aldrich, and Fluka, ensuring high-grade purity, and employed without any purification processes. The solutions were prepared using ultrapure water. The NMR spectra were meticulously recorded by using a Bruker 400 MHz instrument, utilizing $CDCl_3$ as the solvent and employing TMS as the standard. FT-IR spectra were obtained using a Shimadzu IR Prestige 21 spectrometer. The melting points of the titled compounds were acquired using a Stuart SMP30.

B. METHODS

B.1. Chemistry

The synthesis of substituted 4-(2,6-diphenylpyridin-4-yl)-2,6-dimethoxyphenol derivatives was realised according to the literature procedure [21] as in Figure 1. For this, 0.5 mmol of syringaldehyde and 1 mmol of methylketone derivatives were dissolved in 5 mL of DMF. 2 mmol of ammonium acetate was added to the reaction mixture. The resulting mixture was stirred for 72 hours at 180 °C then poured onto 200 mL of ice water, further work up was made with DCM followed by evaporation of the solvent. The crude oily products have been recrystallized from hexane-dichloromethane solvent system.

1 (Syringaldehyde)   **2a-h** (Ketones)   **(3a-h)**

$$Ar = \quad -C_6H_4\text{-}CH_3, \quad -C_6H_4\text{-}Cl, \quad -C_6H_4\text{-}OCH_3, \quad -C_6H_5,$$
$$-C_6H_4\text{-}Br, \quad -C_4H_3S \quad -C_6H_4\text{-}C_6H_5, \quad -C_7H_7NO$$

Scheme 1. Synthesis of 2,4,6-triarylpyridines.

B.2. Antioxidant activity

B.2.1. DPPH Assay

The antioxidant property of the compounds (**3a-h**) was evaluated based on the change in color of the methanolic solution of DPPH, from deep violet to yellow upon adding the compounds. The title compounds' free radical scavenging abilities were assessed by a modified version of the DPPH assay, which was originally described by Blois back in 1958 [22]. In this assay, 3 mL of the compound solution

at various concentrations (5-100 µg/mL) were added to 1 mL of a DPPH solution (0.26 mM solution in methanol). The mixtures were thoroughly vortexed and then incubated at room temperature for 30 minutes in the dark. Following the incubation period, the absorbance of each mixture was measured at a wavelength of 517 nm. The measured absorbance values were subsequently converted to % activity, and the IC$_{50}$ (µg/mL) concentrations of the studied compounds were calculated. Furthermore, a comparison was made between the obtained results and those of Trolox, a reference compound employed in this study.

B.2.2. ABTS Assay

The cationic radical scavenging activities of studied compounds were determined using a modified version of the method originally outlined by Re et al. in 1999 [23]. For the assay, a 2 mM solution of ABTS (2,2'-Azino-bis 3-ethylbenzothiazoline-6-sulfonic acid) and a 2.45 mM solution of $K_2S_2O_8$ (potassium persulfate) were diligently prepared in a 0.1 M phosphate buffer with a pH of 7.4. Subsequently, the two solutions were combined in a precise 1:2 ratio, and the resultant mixture was kept in a light-protected environment for a duration of 12 hours. For the experimental procedure, the compounds and standards to be tested were prepared as stock solutions with a concentration of 1 mg/ml. Samples were extracted in different quantities: 20, 40, 80, 120, 160, 240, 320, and 400 µl, and the volumes were subsequently adjusted to 3 ml with phosphate buffer. Afterward, 1 ml of the ABTS$^{+\bullet}$ solution was added to each sample. The resulting mixture was vigorously vortexed to ensure proper mixing and then incubated at room temperature for a duration of 60 minutes. After the designated incubation period, the absorbance of each mixture was measured at a wavelength of 734 nm. The acquired absorbance values were subsequently converted into percentage activity. The IC$_{50}$ values (µg/mL) were determined for each sample correspondingly, and a comparative analysis was conducted with Trolox, which served as the reference substance in this study.

B.2.3. FRAP Assay

To prepare the sample solutions, a 100 µl volume of each solution, with a concentration of 1 mg/mL, was diluted to 1.25 mL using a phosphate buffer (0.2 M, pH 6.6). Following this, 1.25 mL of potassium ferric cyanide [$K_3Fe(CN)_6$] solution (1%) was added, and the resulting mixture was incubated at 50 °C for a duration of 20 minutes. After the incubation period, 1.25 mL of 10% trichloroacetic acid (TCA) and 0.25 mL of 0.1% $FeCl_3$ solution were introduced into the reaction medium. The absorbance of the final mixture was measured at 700 nm. The antioxidant capacity of the samples was expressed as milligrams (mg) of Trolox equivalent (TE) per gram (g) of the compound. The findings of this study contribute valuable insights into the antioxidant potential of the compounds under investigation.

B.3. Computational Methodology

Computational chemistry provides an enormous role for better understanding the electronic nature of the titled compounds, for instance, DFT calculations were carried out using ORCA 5.0.2 [24] an open-source DFT code. Entire calculations were performed using B3LYP theory [25-28] with def2-SVP def2-TZVP basis sets [29] and Grimme's dispersion correction D3 [30] along with Becke-Johnson damping [31], RIJCOSX approximation [32] and auxiliary basis set [33]. To gain a deeper understanding of the compound's behavior, the C-PCM (Continuum-PCM) solvation model was utilized, simulating the compound's solvation in water. This step was performed subsequent to completing the calculations in the gas phase [34]. The obtained data was visualized by Avogadro 1.2.0 and IboView graphical user interface programs [35-38]. No imaginary frequencies were observed which declare the true minima of optimization energy. The xyz coordinates of the optimized structure were applied to obtain the energies of each system in anion and cation forms. The obtained data were used to compute the vertical ionization potential (I) and electron affinity (A) from the following formulas, respectively.

$$I = E(N - 1) - E(N) \tag{1}$$

and

$$A = E(N) - E(N + 1) \tag{2}$$

E(N) refers to the energy of a system in its neutral form, while E(N-1) to the energy of its cationic form, and E(N + 1) for the corresponding anionic form. Based on these results, the electron-donating ($\omega-$) and electron-accepting ($\omega+$) powers [39] were determined for the studied compounds based on the following formulas:

$$\omega- = \frac{(3I + A)^2}{16(I - A)} \tag{3}$$

$$\omega+ = \frac{(I + 3A)^2}{16(I - A)} \tag{4}$$

Donor and acceptor indexes are usually used to normalize the electron donating-accepting powers giving a useful graphic indicator comparing to Na and F atoms respectively. The obtained data was carried out using computational values done at the same level of theory and the same basis sets.

$$R_d = \frac{\omega -}{\omega + _F} \tag{5}$$

$$R_a = \frac{\omega +}{\omega + _F} \tag{6}$$

The indices R_d (electron donation index) and R_a (electron acceptor index) are fundamental in characterizing electron donation and acceptance capabilities of compounds. R_d quantifies the ability of a compound to donate electrons, while R_a represents its capacity to accept electrons. The reference atoms for R_d and R_a are sodium and fluorine, respectively. Compounds exhibiting a donor index (R_d) value of 1 are classified as electron donors akin to the sodium atom. Donor indices below 1 indicate compounds that are effective electron donors, while values above 1 suggest less effectiveness compared to sodium. Similarly, R_a values greater than 1 indicate compounds that are efficient electron acceptors, with a R_a value of 1 representing acceptor efficiency similar to fluorine. Conversely, R_a values below 1 signify compounds that are less effective electron acceptors than fluorine. By evaluating both R_d and R_a values, the electron donor-acceptor properties of molecules can be comprehensively understood, enabling the classification of compounds as good-poor electron donors-acceptors. Moreover, an acceptor-donor map was constructed by utilizing the R_d and R_a values of the synthesized compounds, which were subsequently compared to the well-known antioxidant Trolox [40]. In summary, the R_d and R_a indices provide valuable insights into the electron donation and acceptance capabilities of compounds. The reference atoms, sodium, and fluorine, aid in determining the relative effectiveness of compounds as electron donors or acceptors. The acceptor-donor map, along with the comparison to Trolox, contributes to a deeper understanding of the electron transfer properties of the synthesized molecules.

B.3.1. The Fukui function f⁻(r)

The Fukui functions are mathematical descriptors that provide information on the electronic density changes of a chemical system in a specific reaction resulting from changes in electron number. These functions can be used to predict the selectivity of regions in the reactions by identifying reactive sites. In this study, the radical Fukui function was used to predict the favorable radical-molecule interaction site in the context of this work [41-45]. Given the nature of the chemical systems studied in this research, the Fukui function was calculated by removal of an electron by using the following formula:

$$f^-(r) = \rho N(r) - \rho N - 1(r) \tag{7}$$

The electron density of the neutral system is denoted as $\rho N(r)$, whereas $\rho N-1(r)$ represents the electron density of the system after the loss of one electron. The obtained results were visualized using the Avogadro 1.2.0 and IboView graphical user interface programs, enabling a visual representation of the electron density distribution and providing a valuable tool for further analysis and interpretation [35-38].

B.3.2. Molecular descriptors evaluation

Based on previously published research, the studied compounds (3a-h) underwent calculations to determine their HOMO (highest occupied molecular orbital) and LUMO (lowest unoccupied molecular orbital) energies, with the lowest values being chosen along with various quantum chemical parameters which were determined accordingly using the proper formula and methodology [46-49, 52]. Tables 2 and 3 present some of the obtained results.

III. RESULTS AND DISCUSSION

A. CHEMISTRY

The title compounds were successfully obtained by the reaction of 1:2:4 equimolar amount of syringaldehyde, methylketone derivatives and ammonium acetate, respectively (Scheme 1). The yields of the synthesized compounds were observed between 60-82%. The structures of the synthesized compounds were elucidated using ^{1}H-NMR, ^{13}C-NMR and FT-IR techniques. For instance, in the spectroscopic data of **3a**, the doublets at δ: 8.08 and 7.68 ppm are correlated to 8 protons of bromophenyl moieties at 2- and 6- positions of the pyridine ring. It can be seen that these protons are resonated as AA'BB' system. The coupling constants are shown as 8.8 Hz which are describing *ortho* couplings. In addition, the singlet at δ: 7.81 ppm is related to two protons of the pyridine ring at 3- and 5- positions. This signal has been shifted downfield due to electron withdrawing effect of the nitrogen atom on the pyridine ring. On the other hand, syringaldehyde-related two aromatic protons appear at δ: 6.93 ppm as singlet. This upfield resonance can be attributed to electron donation properties of hydroxyl and methoxy groups. Finally, the methoxy group protons with 6 integration value have been resonated as a singlet at δ: 4.03 ppm as expected. In the ^{13}C-NMR spectrum of **3a**, the aromatic region has eleven signals according to the proposed structure. Based on the symmetry of the title compound, most of the signals get longer in length due to the overlap of the related signals. Specifically, methoxy carbons resonated at δ: 56.60 ppm as expected. In the FTIR spectrum of **3a**, aromatic C-H and aliphatic C-H stretches are shown at 3419, 2960, and 2937 cm^{-1} values. In addition, aromatic C=C are present in 1598 cm^{-1} region. As a result, the spectroscopic data verified the proposed structure of **3a**. According to the obtained spectroscopic data of the other compounds, all the structures of title compounds are similarly verified as in Figure 2.

A.1. Spectral Data of the Synthesized Compounds

A.1.1. 4-(2,6-bis(4-bromophenyl)pyridin-4-yl)-2,6-dimethoxyphenol (3a)

Yield: 60% pale brown solid, m.p.: 200-205 °C, ^{1}H-NMR (400 MHz, CDCl$_3$, ppm): δ: 8.08 (d, 4H, *j*: 8.8 Hz); 7.81 (s, 2H); 7.68 (d, 4H, *j*: 8.8 Hz); 6.93 (s, 2H); 5.76 (bs, 1H); 4.03 (s, 6H). ^{13}C-NMR (100 MHz, CDCl$_3$, ppm): δ: 156.39 (2C), 150.85, 147.63 (2C), 138.22 (2C), 136.04, 131.88 (4C), 130.13, 128.69 (4C), 123.66 (2C), 116.96 (2C), 104.13 (2C), 56.60 (2C). FTIR (ATR, cm^{-1}): 3419, 2960, 2937, 1598, 1519, 1211, 1114, 1006, 819.

A.1.2. 4-(2,6-bis(4-chlorophenyl)pyridin-4-yl)-2,6-dimethoxyphenol (3b)

Yield: 65%, brown solid, m.p.: 146-149 °C, ^{1}H-NMR (400 MHz, CDCl$_3$, ppm): δ: 8.14 (d, *j* = 8.4 Hz, 4H); 7.80 (s, 2H); 7.50 (d, *j*: 8.4 Hz, 4H); 6.93 (s, 2H), 5.75 (bs, 1H), 4.04 (s, 6H). ^{13}C-NMR (100 MHz, CDCl$_3$, ppm) δ: 156.35 (2C), 150.83, 147.63 (2C), 137.81 (2C), 135.30 (2C), 130.22, 128.92 (4C), 128.39 (5C), 116.93 (2C), 104.13 (2C), 56.61 (2C). FTIR (ATR, cm^{-1}): 3419, 2941, 1716, 1653, 1598, 1519, 1456, 1381, 1359, 1213, 1114, 819.

A.1.3. 4-(2,6-di-p-tolylpyridin-4-yl)-2,6-dimethoxyphenol (3c)

Yield: 79%, brown solid, m.p.: 98-103 °C, ^{1}H NMR (400 MHz, CDCl$_3$, ppm) δ: 8.11 (d, j: 7.8 Hz, 4H); 7.78 (s, 2H), 7.34 (d, j= 7.8 Hz, 4H), 6.95 (s, 2H), 5.74 (bs, 1H), 4.03 (s, 6H), 2.46 (s, 6H). ^{13}C-NMR (100 MHz, CDCl$_3$, ppm) δ: 157.43 (2C), 150.29, 147.54 (2C), 139.01(2C), 136.93(2C), 130.80, 129.42 (4C), 129.31, 127.03(4C), 116.40(2C), 104.11(2C), 56.56(2C), 21.35(2C). FTIR (ATR, cm^{-1}): 3419, 2918, 1716, 1653, 1598, 1508, 1456, 1211, 1111, 817, 570.

A.1.4. 4-(2,6-bis(4-methoxyphenyl)pyridin-4-yl)-2,6-dimethoxyphenol (3d)

Yield: 69%, brown solid, m.p.: 90-96 °C, ^{1}H NMR (400 MHz, CDCl$_3$, ppm) δ: 8.17 (d, j: 8.8 Hz, 4H), 7.71 7.71 (s, 2H), 7.06 (d, j: 8.8 Hz, 4H), 6.94 (s, 2H), 5.81 (bs, 1H), 4.01 (d, 6H), 3.91 (d, 6H). ^{13}C-NMR (100 MHz, CDCl$_3$, ppm) δ: 160.54(2C), 157.01(2C), 150.21, 147.53(2C), 144.69, 132.42 (2C), 130.62, 128.44(4C), 115.55(2C), 114.09(4C), 104.14(2C), 56.55(2C), 55.40(2C). FTIR (ATR, cm^{-1}): 3354, 2935, 1697, 1653, 1597, 1508, 1456, 1247, 1111, 819, 582.

A.1.5. 4-(2,6-diphenylpyridin-4-yl)-2,6-dimethoxyphenol (3e)

Yield: 70%, brown solid, m.p.: 96-100 °C, ^{1}H NMR (400 MHz, CDCl$_3$, ppm) δ: 8.22 (d, j: 8.8 Hz, 4H), 7.84 (s, 2H), 7.56 (t, j: 8.8 Hz, 4H), 7.48 (t, j: 8.8 Hz, 2H), 6.97 (s, 2H), 4.03 (s, 6H). ^{13}C-NMR (100 MHz CDCl$_3$,, ppm) δ: 157.56(2C), 150.47, 147.57(2C), 139.64(2C), 135.81, 130.60, 129.10(2C), 128.75 (4C), 127.19(4C), 117.02(2C), 104.10(2C), 56.57(2C). FTIR (ATR, cm^{-1}): 3315, 2935, 1714, 1645, 1595, 1516, 1448, 1396, 1213, 775, 692, 642.

A.1.6. 4-(2,6-di([1,1'-biphenyl]-4-yl)pyridin-4-yl)-2,6-dimethoxyphenol (3f)

Yield: 75%, brown solid, m.p.: 97-103 °C, ^{1}H NMR (400 MHz, CDCl$_3$, ppm) δ: 8.32 (d, j: 7.8 Hz, 4H), 7.89 (s, 2H), 7.80 (d, j: 7.8 Hz, 4H), 7.72 (d, j: 7.8 Hz, 4H), 7.50 (d, j: 7.8 Hz, 4H), 7.42 (t, 8.0 Hz, 2H) 7.00 (s, 2H), 4.05 (s, 6H). ^{13}C-NMR (CDCl$_3$, 100 MHz, ppm) δ: 157.16 (2C), 150.45, 147.67 (2C), 141.86 (2C), 140.69(2C), 138.55(2C), 130.44, 128.88 (4C), 127.59(4C), 127.44(4C), 127.28, 127.23, 127.13(4C), 116.96(2C), 104.30 (2C), 56.62(2C). FTIR (ATR, cm^{-1}): 3307, 2935, 1647, 1597, 1514, 1448, 1390, 1309, 1112, 1006, 839, 765, 694, 594.

A.1.7. 4-(2,6-di(thiophen-2-yl)pyridin-4-yl)-2,6-dimethoxyphenol (3g)

Yield: 82%, brown solid, m.p.: 100-106 °C, ^{1}H NMR (400 MHz, CDCl$_3$, ppm) δ: 7.74 (dd, j: = 3.7, 4.0 Hz, 2H), 7.63 (s, 2H), 7.46 (dd, j: 5.0, 4.0 Hz, 2H), 7.17 (dd, j: = 5.0, 3.7 Hz, 2H), 6.92 (s, 2H), 4.03 (s, 6H). ^{13}C NMR (100 MHz, CDCl$_3$, ppm) δ: 152.47(2C), 150.44, 147.56(2C), 144.73(2C), 135.96, 129.94(2C), 127.96(2C), 127.88(2C), 124.84(2C), 114.85(2C), 104.04(2C), 56.56(2C). FTIR (ATR, cm^{-1}): 3336, 2935, 1714, 1699, 1647, 1595, 1514, 1411, 1390, 1355, 1213, 1111, 1039, 1006, 829, 698.

A.1.8. 4-([2,2':6',2''-terpyridin]-4'-yl)-2,6-dimethoxyphenol (3h)

Yield: 78%, brown solid, m.p.: 89-95 °C, ^{1}H NMR (400 MHz, CDCl$_3$, ppm) δ: 8.82-8.74 (m, 4H), 8.66 (s, 2H), 7.92-7.88 (m, 2H), 7.42-7.36 (m, 2H), 7.11 (s, 2H), 4.01 (s, 6H). ^{13}C NMR (100 MHz, CDCl$_3$, ppm) δ: 155.73(2C), 150.50, 149.01(2C), 148.33(2C), 147.58 (2C), 137.05(2C), 126.54, 123.90(2C), 122.50, 121.58(2C), 118.62(2C) 104.23(2C), 56.50(2C). FTIR (ATR, cm^{-1}): 3307, 2935, 1714, 1695, 1593, 1514, 1456, 1390, 1361, 1328, 1213, 1112, 1041, 831, 767, 696.
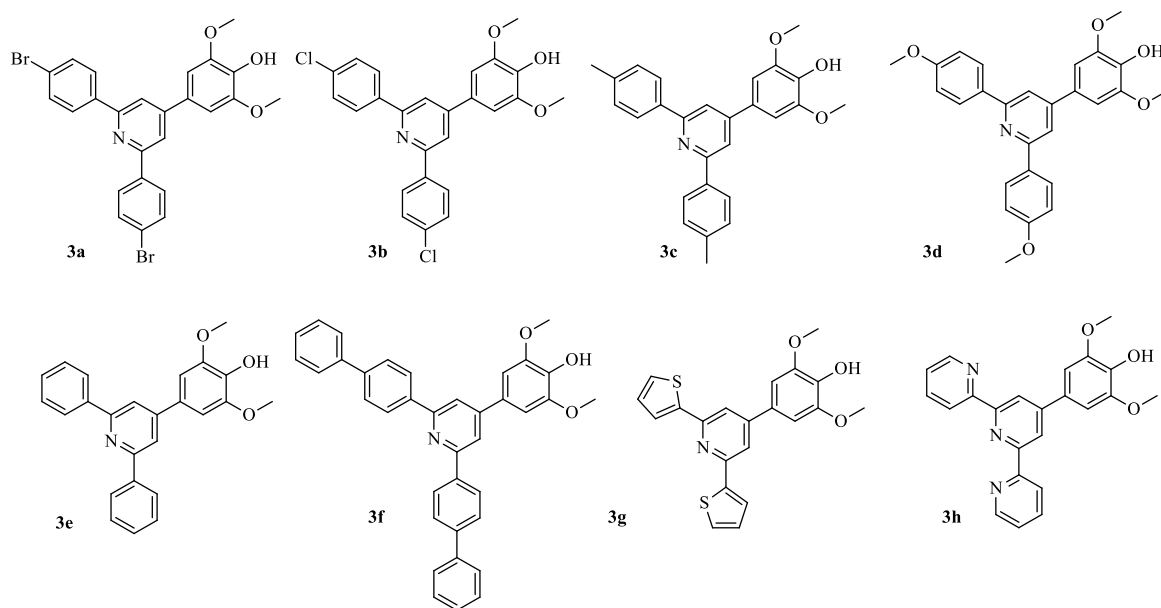
Figure 2. The chemical structures of the studied compounds (3a-h)

B. ANTIOXIDANT ACTIVITY

B.1. Antioxidant activity by ABTS

The ABTS cation radical decolorization assay is a widely used method to assess the antioxidant activity of various compounds. Additionally, Trolox is commonly employed as a reference compound in this assay. Table 1 showed that in general IC_{50} of the studied compounds were between 51.26 and 148.75 µg/mL where Trolox has 7.07 µg/mL IC_{50} value. According to the obtained experimental results, the methyl group containing derivative (**3c**) has the lowest IC_{50} value. The standard and the studied compounds showed the antioxidant ability in the following order: 3f<3e<3g<3b<3a<3d<3h<3c<Trolox Figure 3 illustrates the activation/concentration dependence of the studied compound.
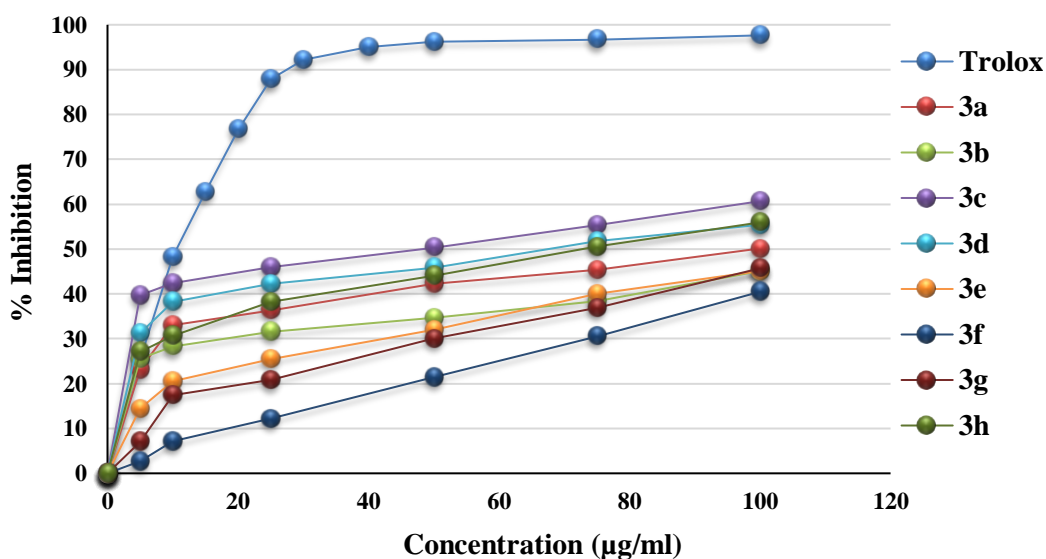

Figure 3. Activation/concentration dependence of the studied compound towards ABTS.

B.2. Antioxidant activity by DPPH

Various methods can be employed to evaluate the radical scavenging capacity of natural and synthetically obtained compounds. Among these, stable DPPH· (2,2-diphenyl-1-picrylhydrazyl) free radical assays are widely utilized due to their simplicity and relatively short analysis time compared to other evaluation methods. In this study, Trolox was used as radical scavenger reference compound. In the DPPH assay, the IC_{50} values of the tested compounds ranged from 124.73 to 285.98 µg/mL, while Trolox exhibited an IC_{50} value consisting of 11.95 µg/mL. **3d** has the lowest IC_{50} value. The standard and the studied compounds showed the ability to scavenge DPPH· in the following order: 3b <3g<3f<3e<3a<3c<3h<3d<Trolox. Figure 4 illustrates the activation/concentration dependence of the studied compound.
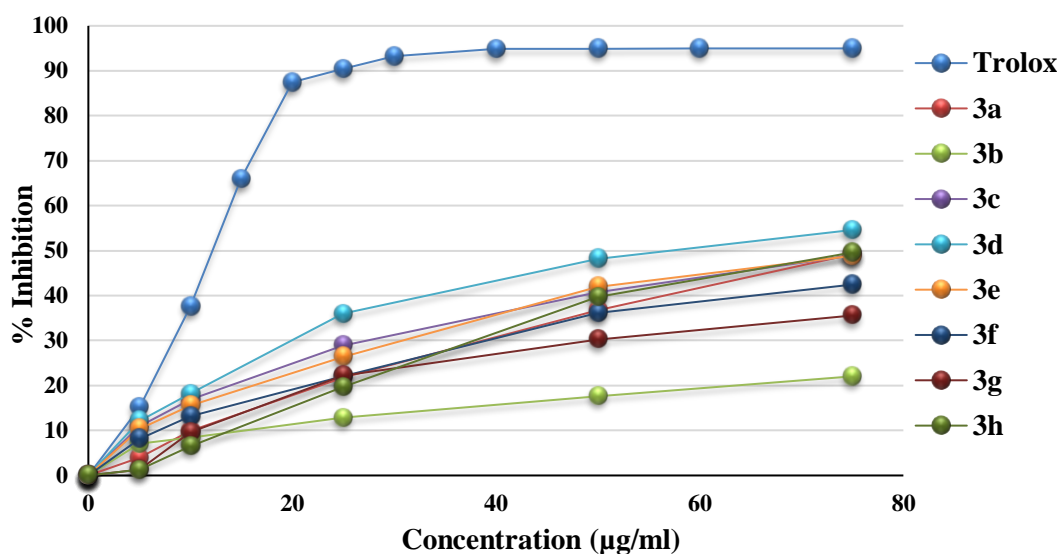

Figure 4. Activation/concentration dependence of the studied compound towards DPPH.

B.3. Antioxidant activity by FRAP

A comparative analysis was performed to assess the ability of the studied compounds to reduce ferric ions, in comparison to the Trolox standard. The chloro derivative (**3b**) had a reducing power of 21.89±0.84 mg Trolox equivalent (TE). The FRP of the bromo derivative (**3a**) was also found 23.32±0.84 µg TE. According to other studies [50, 51], our findings were consistent with these studies. Figure 5 illustrates the activation/concentration dependence of the studied compound.
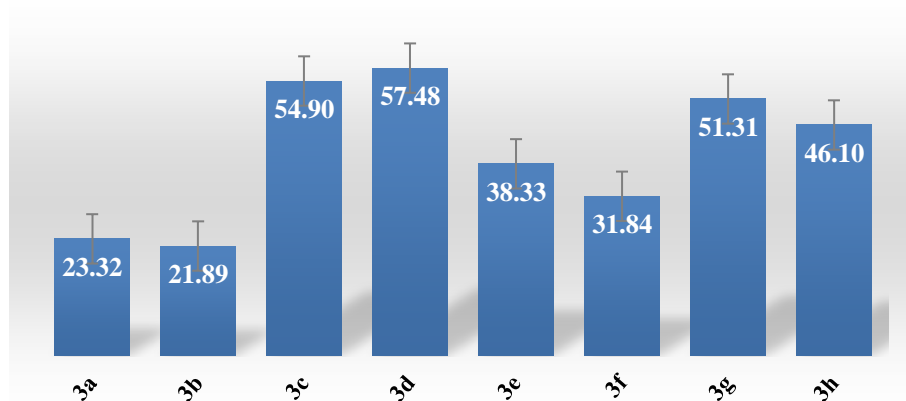

Figure 5. Activation/concentration dependence of the studied compound towards FRAP.

C. THEORETICAL STUDIES

The optimized structures for the ground state were obtained using the B3LYP def2-TZVP level of theory in both the gas phase and water. The initial geometric optimization was carried out in the def2-SVP basis set. Furthermore, the utilization of quantum chemical calculations to estimate molecular parameters is an effective technique for comprehending a molecule's activities. These calculations provide valuable insights into the electronic structure, stability, and reactivity of the molecules, contributing to a better understanding of their properties and potential applications. Quantum chemical parameters, such as E_{HOMO}, E_{LUMO}, Δ_E (the energy difference between HOMO and LUMO), hardness, electronegativity, chemical potential, global electrophilicity, nucleophilicity, global softness, dipole moments, ionization energies, and electron affinities, can all be considered when evaluating the biological potential of a molecule [52]. One can observe by looking at the given Table 1 which contains some calculated parameters for the studied compounds along with the data of Figure 6 that **3a-h** compounds have similar or near energy band gap energy difference (Δ_E) in gas phase. It can be seen also from Table 1 that the studied compounds showed a slightly small changed in Δ_E using B3LYP theory under gas phase. Chemical hardness values seem to be considerably good among the studied theory and it could contribute to the antioxidant mechanism. Moreover, the outputs which been observed in Table 2 as water CPCM system with dielectric constant value of 80.4 clearly declare that the (Δ_E) of studied compounds were between 3.961 and 4.273 eV, also the obtained ionization potential (I) and electron affinity values as 5.74 - 5.751 and 1.446 - 1.779 respectively which plays a crucial role in understanding the antioxidant properties and the nature of the studied compounds and their ability to scavenge free radicals. In general, the antioxidant capacity of a molecule can be defined by taking into account both ionization potential and electron affinity. Compounds with favorable ionization potentials and electron affinities have high antioxidative characteristics ability, allowing them to efficiently counteract oxidative stress and the damage it causes. The related HOMO-LUMO band gap map (Frontier Molecular Orbitals) can be seen in Figure 7.
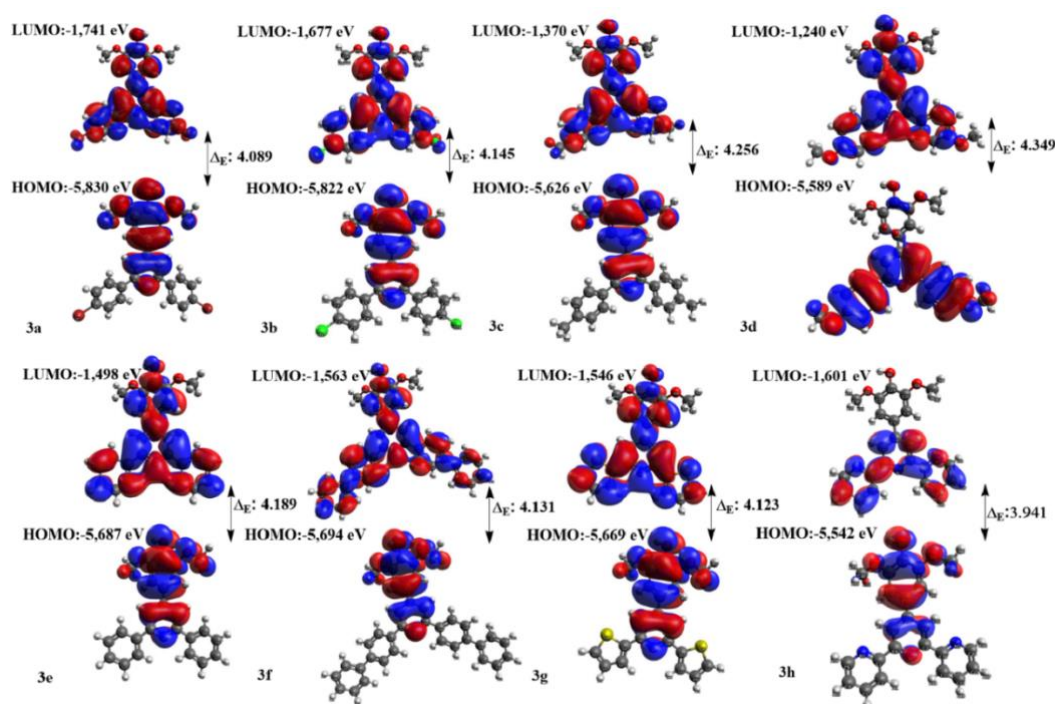

Figure 6. *Calculated HOMO-LUMO band gap map (Frontier Molecular Orbitals) of the studied compounds under gas phase.*

Table 1. *Calculated parameters of the studied compounds (3a-h) under gas phase*

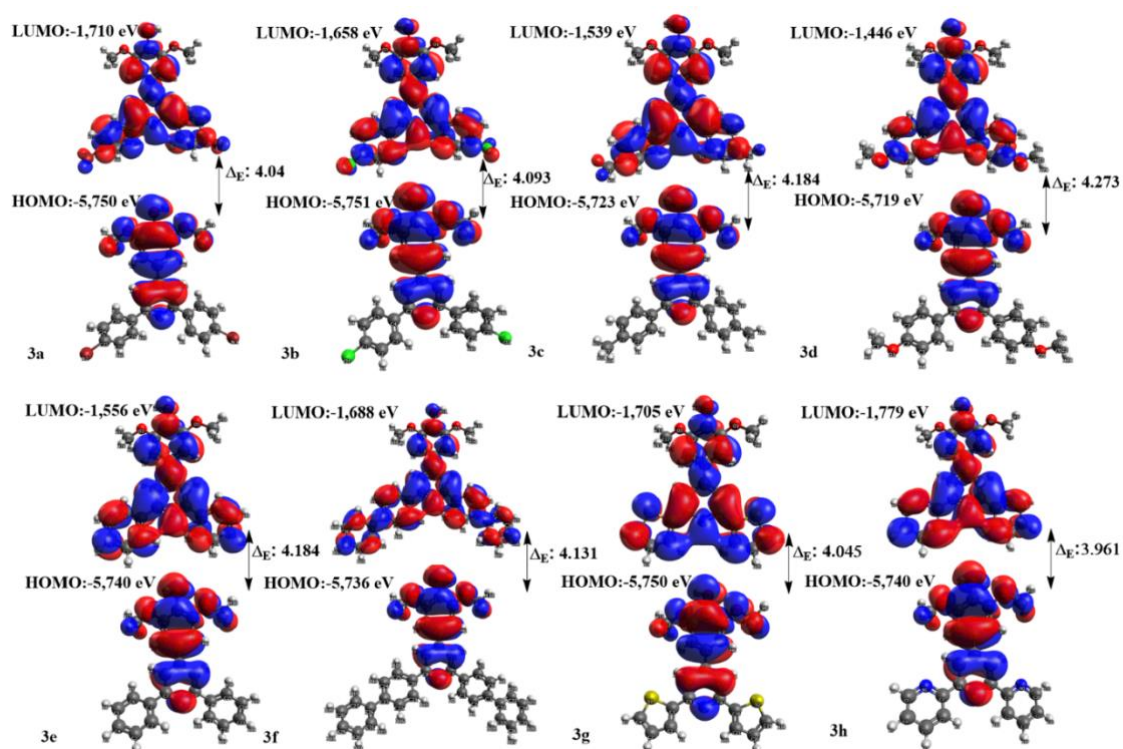| Sample	E_{HOMO}	E_{LUMO}	Δ_E	ω^-	ω^+	I	A	Ra	Rd
3a	-5.83	-1.741	4.089	9.829	5.649	5.830	1.71	0.119	1.071
3b	-5.822	-1.677	4.145	9.918	5.623	5.822	1.677	0.118	1.081
3c	-5.626	-1.370	4.256	9.707	5.179	5.626	1.37	0.109	1.058
3d	-5.589	-1.240	4.349	9.789	5.060	5.589	1.24	0.106	1.067
3e	-5.687	-1.498	4.189	9.717	5.331	5.687	1.498	0.112	1.059
3f	-5.694	-1.563	4.131	9.627	5.361	5.694	1.563	0.113	1.049
3g	-5.669	-1.546	4.123	9.561	5.311	5.669	1.546	0.112	1.042
3h	-5.542	-1.601	3.941	8.979	5.096	5.542	1.601	0.107	0.979
Trolox	-5.336	-0.107	5.229	10.533	3.697	5.336	0.107	0.078	1.148

Figure 7. *Calculated HOMO-LUMO band gap map (Frontier Molecular Orbitals) of the studied compounds using water.*

Table 2. *Calculated parameters of the studied compounds (3a-h) using water.*

Sample	E_{HOMO}	E_{LUMO}	Δ_E	ω^-	ω^+	I	A	Ra	Rd
3a	-5.750	-1.710	4.040	9.574	5.494	5.750	1.71	0.115	1.044
3b	-5.751	-1.658	4.093	9.675	5.487	5.751	1.658	0.115	1.055
3c	-5.723	-1.539	4.184	9.784	5.407	5.723	1.539	0.114	1.066
3d	-5.719	-1.446	4.273	9.936	5.371	5.719	1.446	0.113	1.083
3e	-5.74	-1.556	4.184	9.819	5.443	5.740	1.556	0.114	1.070
3f	-5.736	-1.688	4.131	9.561	5.464	5.736	1.688	0.115	1.042
3g	-5.750	-1.705	4.045	9.584	5.493	5.75	1.705	0.115	1.045
3h	-5.740	-1.779	3.961	9.406	5.484	5.74	1.779	0.115	1.025
Trolox	-5.424	-0.147	5.277	10.830	3.868	5.424	1.71	0.081	1.181

On the other hand, electron affinity plays an important role in antioxidants, which is relevant because antioxidants function by donating electrons to free radicals or reactive oxygen species (ROS), thereby neutralizing their damaging effects. Free radicals are highly reactive species that contain unpaired electrons. They are generated as byproducts of various physiological processes or through external factors such as exposure to pollutants or radiation. These free radicals can cause oxidative stress by initiating chain reactions that damage cellular components, leading to various diseases and aging. By looking at the obtained data from Tables 1 and 2, it can be said that the electron affinity of the studied compounds was between 1.779-1.24 in gas phase compared to (Trolox 0.147) and between 1.779-1.446 in water. Furthermore, ionization energy plays a significant role in the context of antioxidant agents as it influences the stability and reactivity of the antioxidant compounds. Typically, higher ionization energy indicates a greater difficulty in removing an electron from the molecule. By examining the ionization energy, one can gain insights into the potential electron transfer processes and the overall antioxidant activity of the compounds. This means that the antioxidant molecule is less likely to donate electrons to free radicals or reactive oxygen species (ROS). Again by looking at the obtained data from Tables 1 and 2, it can be seen that the ionization values of the studied compounds were between 5.83-5.542 and 5.750-5.719 in gas phase and water, respectively.

C.1. Donor-Acceptor Maps and Fukui function

Donor and acceptor map (DAM) is a widely used helpful tool to predict the free radical stabilizing ability of a compound. This is achieved by either donating electrons (known as an antioxidant), accepting electrons (known as an anti-reductant), or sometimes both (Figure 8). The mentioned mechanisms play a crucial role in stabilizing free radicals, which prevents them from reacting with various bioactive molecules. The significance of scavenging free radicals in the medical field stems from its capacity to mitigate oxidative stress, a known contributor to cell damage and neurodegenerative disorders. [53, 54] The obtained DAM values (Ra and Rd) are shown in Table 1 and 2. Based on these data in gas phase, one can observe that **3h** was a good antiradical compound among the series while other compounds were defined as a less effective electron acceptor than F atom and less effective electron donor than Na atom relatively following the good antioxidant power rate **3h>3g>3f>3e>3c>3d>3a>3b** respectively.
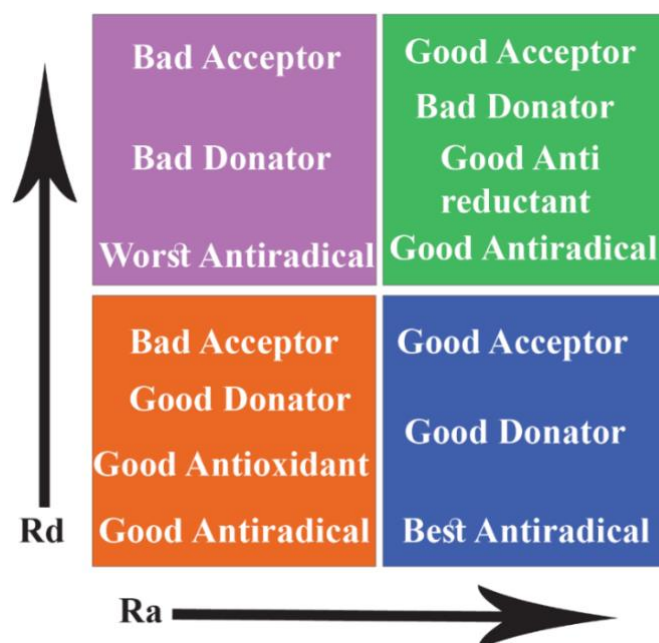

Figure 8. Distinct areas in Electron Donor-Acceptor Map

Through the application of Fukui functions, it becomes feasible to predict the local reactivity of distinct regions within molecules, providing relevant insights into the reactive sites and the types of biochemical

992

reactions in which the studied compounds may participate; in another way, the f$^+$ Fukui function, which pertains to the LUMO orbital, serves as an indicator of the molecule's nucleophilic susceptibility. Conversely, the f$^-$ Fukui function, associated with the HOMO orbital, serves as an indicator of its electrophilic susceptibility. The combined average of the f$^+$ and f$^-$ Fukui functions approximates the susceptibility to radical electron transfer in a studied system. The Fukui theory presents a pragmatic and straightforward approach for calculating chemical information, particularly in the context of early transition states. It provides a realistic framework to analyze and understand the behavior of molecules during chemical reactions, shedding light on their reactivity and the factors influencing their susceptibility to nucleophilic and electrophilic attacks. At the end the utilization of the Fukui function projection onto the van der Waals surface has demonstrated its efficacy in facilitating effective communication and information exchange with different disciplines. This approach serves as a valuable tool to bridge, enabling a clearer understanding and meaningful discussions regarding chemical phenomena and interactions in a studied system. In this manner, Table 3 shows the Fukui indices evaluated using Hirshfeld population analysis obtained using B3LYP theory and def-2 TZVP base set in gas phase. As it is observed that high f^0 values which are associated mostly with the first highest values of oxygen atoms associated with OH groups, for some derivatives it was observed based on the radical Fukui function that the atoms with high F^0 values following associate oxygen atom with OH group were nearly same in value in both water and gas phase and based on the studied theory and basis sets limitations, it can be relatively accepted which clearly contribute to the antioxidant radically attacking position. For instance, by looking at Table 3 under gas phase it can be observed that in **3a** compound, O22 atom was associated with the highest F^0 values which is underlined with bold **0.322782** which indicates the higher ability for a possible radical attack to occur at this position. The same trends were observed for the other studied compounds as well.
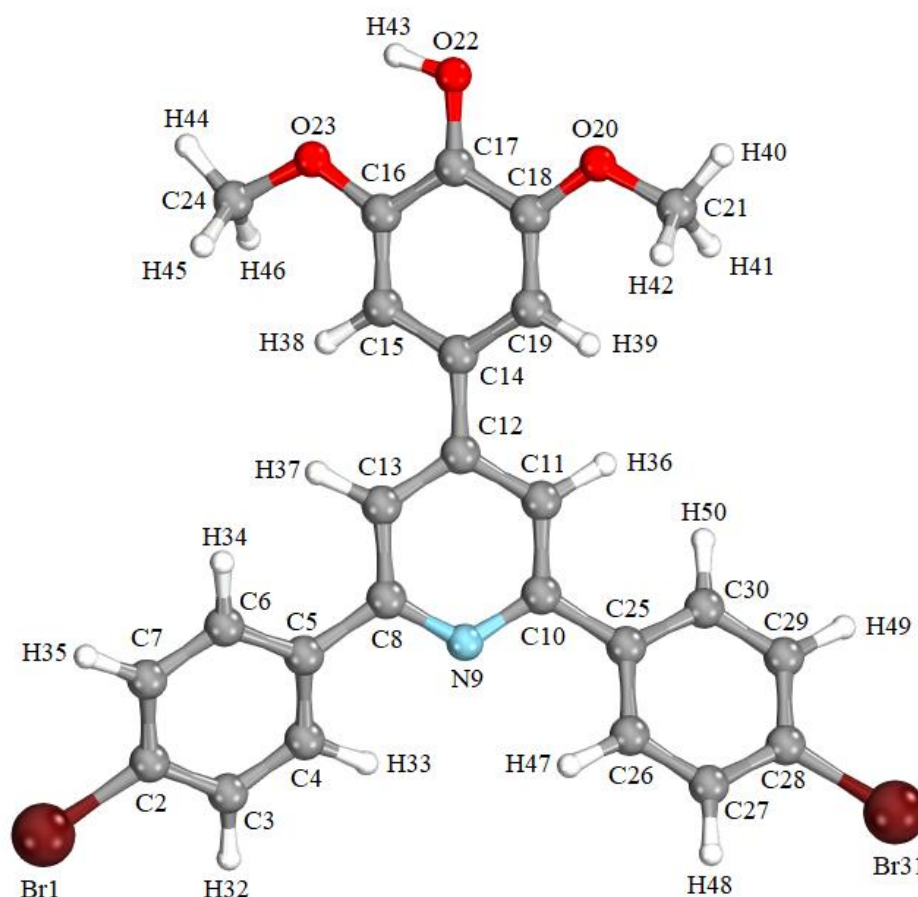

Figure 9. *Atom numbering of 3a*

Table 3. *Fukui functional results for* **3a**.

Atom	Fukui Indices		
	(f⁻)	**(f⁺)**	**(f⁰)**
Br-1	-0.13679	0.00615	0.279724
C-2	-0.00346	0.042246	0.04916
C-3	-0.05134	-0.016436	0.086236
C-4	-0.0423	-0.009302	0.075302
C-5	-0.0043	0.006664	0.015254
C-6	-0.04214	-0.019601	0.064677
C-7	-0.05977	-0.022576	0.096972
C-8	0.025754	0.083969	0.032461
N-9	-0.23645	-0.152105	0.320785
C-10	0.02645	0.083512	0.030612
C-11	-0.06858	-0.035968	0.101198
C-12	-0.03541	0.024757	0.095577
C-13	-0.06827	0.002244	0.13879
C-14	-0.02116	0.027887	0.070201
C-15	-0.09104	-0.047457	0.134619
C-16	0.044277	0.085636	-0.002918
C-17	0.024585	0.114863	0.065693
C-18	0.054461	0.103246	-0.005676
C-19	-0.08933	-0.052339	0.126313
O-20	-0.15214	-0.101422	0.20286
C-21	0.017395	0.039143	0.004353
O-22	-0.22459	-0.126406	**0.322782**
O-23	-0.15202	-0.117518	0.186528
C-24	0.019095	0.038497	0.000307
C-25	-0.00361	0.009016	0.016226
C-26	-0.04181	-0.008498	0.07512
C-27	-0.05117	-0.017894	0.084438
C-28	-0.00267	0.042836	0.048176
C-29	-0.05907	-0.020759	0.097381
C-30	-0.04121	-0.018138	0.064278
Br-31	-0.13588	0.008303	0.280071
H-32	0.028904	0.055527	-0.002281
H-33	0.025099	0.04579	-0.004408
H-34	0.027046	0.040952	-0.01314
H-35	0.025793	0.052925	0.001339
H-36	0.015422	0.04023	0.009386
H-37	0.014826	0.045478	0.015826
H-38	0.01969	0.044366	0.004986
H-39	0.019548	0.043455	0.004359
H-40	0.032393	0.06297	-0.001816
H-41	0.026591	0.04502	-0.008162
H-42	0.025435	0.04265	-0.00822
H-43	0.141838	0.181928	-0.101748
H-44	0.029941	0.045522	-0.01436
H-45	0.028736	0.042922	-0.01455
H-46	0.032458	0.061659	-0.003257
H-47	0.025251	0.045649	-0.004853
H-48	0.029005	0.055136	-0.002874
H-49	0.026327	0.05335	0.000696
H-50	0.027874	0.042209	-0.013539

IV. CONCLUSION

Eight novel 2,4,6-triarylpyridines derived from syringaldehyde were designed and successfully synthesized via a multicomponent one-step preparation method. The structures of all the title compounds (**3a-h**) have been illuminated by FTIR and NMR spectroscopic techniques. Those compounds were evaluated for their antioxidant activities comparing with a known reference compound, Trolox. The studied compounds exhibited considerable antioxidant effects in all the studied assays. In particular, three title derivatives (**3c, 3d, 3h**) exhibited the highest antioxidant activities among the studied series. In addition, by using the B3LYP theory and SVP, TZVP basis sets in DFT studies, a comprehensive theoretical quantum computing approach for the synthesized compounds was established and electronic structure descriptive parameters called Fukui indices associated with the radical scavenging potential were determined. Finally, the structure-activity relationship was revealed by comparing the theoretical and experimental results. The proposed antioxidant activity mechanism of the obtained compounds was supported by Fukui function results. According to the obtained radicalic Fukui indice value (f^0), the highest value associated with the OH functional group in **3a** could explain the antioxidant mechanism of **3a** occurring on this oxygen atom. This approach can serve as a good explaining way for the antioxidant mechanism of similar compounds.

V. REFERENCES

[1] J. D. Hayes, A.T. Dinkova-Kostova, K. D. Tew, "Oxidative stress in cancer", Cancer Cells, vol. 38, pp. 167-197, 2020.

[2] A. M. Pisoschi, A. Pop, F. Iordache, L.Stanca, G. Predoi, A. I. Serban, "Oxidative stress mitigation by antioxidants-an overview on their chemistry and influences on health status", European Journal of Medicinal Chemistry, vol. 209, 112891, 2021

[3] M. V. Irazabal, V. E. Torres, "Reactive oxygen species and redox signaling in chronic kidney disease", Cells, vol. 9, 1342, 2020

[4] H. Sies, D. P. Jones, "Reactive oxygen species (ROS) as pleiotropic physiological signalling agents", Nature Reviews Molecular Cell Biology, vol. 21, pp. 363-383, 2020

[5] N. Zhang, P. Hu, Y. Wang, Q. Tang, Q. Zheng, Z. Wang, Y. He, "A reactive oxygen species (ROS) activated hydrogen sulfide (H2S) donor with self- reporting fluorescence", ACS Sensors, vol. 5, pp. 319-326, 2020

[6] Singh A, Kukreti R, Saso L, Kukreti S. Oxidative Stress: A Key Modulator in Neurodegenerative Diseases. Molecules.; vol. 24(8), pp. 1583, 2019.

[7] Bartosz, G. Reactive oxygen species: Destroyers or messengers?, Biochemical Pharmacology, Vol77,(8), pp.1303-1315, 2009.

[8] Xu, D., Hu, M.J., Wang, Y.Q., Cui, Y.L. Antioxidant Activities of Quercetin and Its Complexes for Medicinal Application. Molecules vol.24, pp.1123, 2019.

[9] Gulcin, I. Antioxidants and antioxidant methods: An updated overview. Arch Toxicol., Vol.94, pp. 651-715, 2020.

[10] D. Yancheva, E. Velcheva, Z. Glavcheva, B. Stamboliyska, A. Smelcerovic, Insights in the radical scavenging mechanism of syringaldehyde and generation of its anion, Journal of Molecular Structure, Vol. 1108, pp. 552-559, 2016.

[11] Chmiel M, Stompor-Gorący M. The Spectrum of Pharmacological Actions of Syringetin and Its Natural Derivatives-A Summary Review. Nutrients. Vol.14(23), pp. 5157, 2022. https://doi.org/10.3390/nu14235157.

[12] Zhou, W.; Yang, L.; Deng, K.; Xu, G.; Wang, Y.; Ni, Q.; Zhang, Y. Investigation of isoflavone constituents from tuber of Apiosamericana Medik and its protective effect against oxidative damage on RIN-m5F cells. Food Chem. Vol. 405, pp.134655, 2023.

[13] Bozkurt, A., Mustafa, G., Tarık, A., Adile, O., Murat, S., Mesut, K., Yıldıray, K., Coskun, S., & Murat, C. Syringaldehyde exerts neuroprotective effect on cerebral ischemia injury in rats through anti-oxidative and anti-apoptotic properties. Neural Regeneration Research. 9(21), pp 1884-1890, 2014. doi: 10.4103/1673-5374.145353

[14] Meshcheryakova, S.A., Kayumova, A.F., Kang, Y., Shumadalova, A., Vinogradova, Y.E., Khuzin, D.A., Ziyakaeva, K.R., Kiseleva, O.D., Gabdulkhakova, I., Beylerli, O., Gareev, I.F., Sufianov, A.A., Sufianova, G.Z., Ahmad, A., Yang, G., & Guo, Z. The Effect Of Whole Blood And Bone Marrow With The Addition Of Pyrimidine-2,4(1h,3h)-Dione Thietanyl Derivatives On Free Radical Oxidation. Curr Med Chem. Vol.30(17), pp.1993-2004, 2023 doi: 10.2174/0929867329666220805125638.

[15] Lee DH, Folsom AR, Harnack L, Halliwell B, Jacobs DR Jr. Does supplemental vitamin C increase cardiovascular disease risk in women with diabetes? Am J Clin Nutr. Vol.80(5), pp.1194-200, 2004. doi: 10.1093/ajcn/80.5.1194. PMID: 15531665.

[16] Akman, T.C, Simsek, S., Kayir, Ö., Zeynep, A., Aksit H., Genc, N. LC-ESI-MS/MS Chemical Characterization, Antioxidant and Antidiabetic Properties of Propolis Extracted with Organic Solvents from Eastern Anatolia Region. Chem. Biodiversity. Vol.20, e202201189, 2023.

[17] Nikolaos Nenadis, Olga Lazaridou, and Maria Z. Tsimidou Journal of Agricultural and Food Chemistry. Vol.55 (14), pp.5452-5460, 2007. doi: 10.1021/jf070473q

[18] Grimme S, Antony J, Schwabe T, Mück-Lichtenfeld C. Density functional theory with dispersion corrections for supramolecular structures, aggregates, and complexes of (bio)organic molecules. Org Biomol Chem. Vol. 5(5), pp.741-58, 2007. doi: 10.1039/b615319b. Epub 2007 Jan 26. PMID: 17315059.

[19] Mendoza Huizar, L. H., Rios-Reyes, C. H., Maturano, O., Robles, J., Rodriguez, J. A. "Chemical reactivity of quinclorac employing the HSAB local principle - Fukui function" Open Chemistry, vol. 13, no. 1, pp. 000010151520150008. 2015. https://doi.org/10.1515/chem-2015-0008

[20] Tasheh, N.S., Fouegue, A.D.T., Ghogomu, J.N., Investigation of the Antioxidant and UV Absorption Properties of 2-(2'-hydroxy-5'-methylphenyl)-benzotriazole and Its Ortho-Substituted Derivatives via DFT/TD-DFT, Comput. Chem. 09 (2021) 161–196. https://doi.org/10.4236/cc.2021.93010.

[21] Kenchappa, Yadav D. Bodke, A. Chandrashekar, Sandeep Telkar, K.S. Manjunatha, M. Aruna Sindhe, Synthesis of some 2, 6-bis (1-coumarin-2-yl)-4-(4-substituted phenyl) pyridine derivatives as potent biological agents, Arabian Journal of Chemistry, Vol. 10, pp. S1336-S1344, 2017.

[22] Marsden S. Blois, Antioxidant Determinations by the Use of a Stable Free Radical, Nature, Vol. 181, pp 1199-1200, 1958.

[23] R Re, N Pellegrini, A Proteggente, A Pannala, M Yang, C Rice-Evans. Antioxidant activity applying an improved ABTS radical cation decolorization assay, Free Radic Biol Med. Vol. 9-10 pp1231-1237, 1999.

[24] Neese, F. Software update: The ORCA program system-Version 5.0, WIREs Comput. Mol. Sci. Vol.12, pp. 1–15, 2022. https://doi.org/10.1002/wcms.1606

[25] Becke, A.D. Density-functional thermochemistry. III. The role of exact exchange, J. Chem. Phys. 98. 5648–5652, 1993. https://doi.org/10.1063/1.464913.

[26 Lee, C., Yang, W., Parr, R.G. Development of the Colle-Salvetti correlation-energy formula into a functional of the electron density, Phys. Rev. B. 37.785–789, 1988. https://doi.org/10.1103/PhysRevB.37.785.

[27] Stephens, P.J., Devlin, F.J., Chabalowski, C.F., Frisch, M.J. Ab Initio Calculation of Vibrational Absorption and Circular Dichroism Spectra Using Density Functional Force Fields, J. Phys. Chem. 98. 11623–11627, 1994 https://doi.org/10.1021/j100096a001.

[28] Vosko, S.H., Wilk, L., Nusair, M. Accurate spin-dependent electron liquid correlation energies for local spin density calculations: a critical analysis, Can. J. Phys. 58. 1200–1211, 1980. https://doi.org/10.1139/p80-159.

[29] Weigend, F., Ahlrichs, R. Balanced basis sets of split valence, triple zeta valence and quadruple zeta valence quality for H to Rn: Design and assessment of accuracy, Phys. Chem. Chem. Phys. 7. pp.3297, 2005. https://doi.org/10.1039/b508541a.

[30] Grimme, S., Antony, J., Ehrlich, S., Krieg, H. A consistent and accurate ab initio parametrization of density functional dispersion correction (DFT-D) for the 94 elements H-Pu, J. Chem. Phys. Vol.132, 154104.2010. https://doi.org/10.1063/1.3382344

[31] Grimme, S., Ehrlich, S., Goerigk, L. Effect of the damping function in dispersion corrected density functional theory, J. Comput. Chem. 32. 1456–1465. 2011. https://doi.org/10.1002/jcc.21759.

[32] Neese, F., Wennmohs, F., Hansen, A., Becker, U. Efficient, approximate and parallel Hartree–Fock and hybrid DFT calculations. A 'chain-of-spheres' algorithm for the Hartree–Fock exchange, Chem. Phys. 356. 98–109. 2009. https://doi.org/10.1016/j.chemphys.2008.10.036.

[33] Weigend, F. Accurate Coulomb-fitting basis sets for H to Rn, Phys. Chem. Chem. Phys. Vol. 8, pp.1057, 2006. https://doi.org/10.1039/b515623h.

[34] Barone, V., Cossi, M. Quantum Calculation of Molecular Energies and Energy Gradients in Solution by a Conductor Solvent Model, J. Phys. Chem. A. Vol. 102, pp.1995–2001, 1998. https://doi.org/10.1021/jp9716997.

[35] Cornell T, Hutchison GR. Version 1.2.0. Avogadro Chemistry; Last modified July 24, 2018. Accessed January 1, 2023. http:// avogadro.cc

[36] Hanwell, M.D., Curtis, D.E., Lonie, D.C., Vandermeersch, T., Zurek, E.,Hutchison, G.R. Avogadro: an advanced semantic chemical editor, visualization, and analysis platform. J Cheminform 4, 17 (2012). https://doi.org/10.1186/1758-2946-4-17

[37] Knizia, G. Intrinsic Atomic Orbitals: An Unbiased Bridge between Quantum Theory and Chemical Concepts. J. Chem. Theory Comput. 9, 4834–4843. 2013.

[38] Knizia, G. & Klein, J. E. M. N. Electron Flow in Reaction Mechanisms—Revealed from First Principles. Angew. Chem. Int. Ed. 54, 5518–5522. 2015.

[39] Gázquez, J.L., Cedillo, A., Vela, A. Electrodonating and Electroaccepting Powers, J. Phys. Chem. A. 111, 1966–1970, 2007. https://doi.org/10.1021/jp065459f.

[40] Zhong, Y., Shahidi, F. 12 - Methods for the assessment of antioxidant activity in foods11This chapter is reproduced to a large extent from an article in press by the authors in the Journal of Functional Foods., in: F.B.T.-H. of A. for F.P. Shahidi (Ed.), Woodhead Publ. Ser. Food Sci. Technol. Nutr., Woodhead Publishing, 2015: pp. 287–333. https://doi.org/https://doi.org/10.1016/B978-1-78242-089-7.00012-9.

[41] Li, Y., Evans, J.N.S. The Fukui Function: A Key Concept Linking Frontier Molecular Orbital Theory and the Hard-Soft-Acid-Base Principle, J. Am. Chem. Soc. 117, 7756–7759, 1995. https://doi.org/10.1021/ja00134a021.

[42] Chattaraj, P.K., Cedillo, A., Parr, R.G. Variational method for determining the Fukui function and chemical hardness of an electronic system, J. Chem. Phys. 103, 7645–7646, 1995. https://doi.org/10.1063/1.470284.

[43] Vela, A., Gazquez, J.L. A relationship between the static dipole polarizability, the global softness, and the fukui function, J. Am. Chem. Soc. 112,1490–1492, 1990. https://doi.org/10.1021/ja00160a029.

[44] Flores-Moreno, R., Melin, J., Ortiz, J. V., Merino, G. Efficient evaluation of analytic Fukui functions, J. Chem. Phys. Vol. 129, 224105, 2008. https://doi.org/10.1063/1.3036926.

[45] Flores-Moreno, R. Symmetry Conservation in Fukui Functions, J. Chem. Theory Comput. Vol.6, 48–54, 2010. https://doi.org/10.1021/ct9002527

[46] Brus, L.E. A simple model for the ionization potential, electron affinity, and aqueous redox potentials of small semiconductor crystallites, J. Chem. Phys. 79, pp.5566–5571, 1983. https://doi.org/10.1063/1.445676.

[47] Cederbaum, L.S., Domcke, W., Schirmer, J., Von Niessen, W., Diercksen, G.H.F., Kraemer, W.P. Correlation effects in the ionization of hydrocarbons, J. Chem. Phys. Vol.69, pp.1591–1603, 1978. https://doi.org/10.1063/1.436733

[48] Szabo A., Ostlund, N. S. Modern Quantum Chemistry Introduction to Advanced Electronic Structure Theory, Dover Publications, New York, 1996.

[49] Parr, R.G., Weitao, Y. Density-Functional Theory of Atoms and Molecules, Oxford University Press, 1995. https://doi.org/10.1093/oso/9780195092769.001.0001.

[50] Cindrić M, Sović I, Mioč M, Hok L, Boček I, Roškarić P, Butković K, Martin-Kleiner I, Starčević K, Vianello R, Kralj, M., Hranjec, M. Experimental and Computational Study of the Antioxidative Potential of Novel Nitro and Amino Substituted Benzimidazole/Benzothiazole-2-Carboxamides with Antiproliferative Activity. Antioxidants. Vol.8(10), pp. 477, 2019, https://doi.org/10.3390/antiox8100477

[51] Soobrattee, M.A., Neergheen, V.S., Luximon-Ramma A., Aruoma O.I., Bahorun T. Phenolics as potential antioxidant therapeutic agents: mechanism and actions. Mutation Research - Fundamental and Molecular Mechanisms of Mutagenesis.Vol.579, pp. 579:200–213, 2005. https://doi.org/10.1016/j.mrfmmm.2005.03.023

[52] Musatat, AB, Atahan, A, Ergün, A, Çıkrıkcı, K, Gençer, N, Arslan, O, et al. Synthesis, enzyme inhibition, and molecular docking studies of a novel chalcone series bearing benzothiazole scaffold. Biotechnol Appl Biochem. Vol.70, pp.1357– 1370, 2023. https://doi.org/10.1002/bab.2445

[53] P.M. Becker, Antireduction: an ancient strategy fit for future, Biosci. Rep. 36 (2016). https://doi.org/10.1042/BSR2016008

[54] Macías-Hernández, E.C., Romero-Chávez, M. M., Mojica-Sánchez, J.P., Pineda-Urbina, K., Martínez, S.T.M., Jimenez-Ruiz, E. I., Via, L. D., Ramos-Organillo, Á. Synthesis and characterization of new monothiooxalamides containing pyridine nuclei with promising antiproliferative and antioxidant activity, Journal of Molecular Structure, Vol.1265, pp.133360, 2022. https://doi.org/10.1016/j.molstruc.2022.133360.